

Strongly Intensive Measures for Multiplicity Fluctuations

V.V. Begun,^{1,2} V.P. Konchakovski,^{1,3} M.I. Gorenstein,^{1,2} and E.L. Bratkovskaya^{4,5}

¹*Bogolyubov Institute for Theoretical Physics, Kiev, Ukraine*

²*Frankfurt Institute for Advanced Studies, Frankfurt, Germany*

³*Institute for Theoretical Physics, University of Giessen, Germany*

⁴*Frankfurt Institute for Advanced Studies, Frankfurt, Germany*

⁵*Institut for Theoretical Physics, University of Frankfurt, Frankfurt, Germany*

Abstract

The recently proposed two families of strongly intensive measures of fluctuations and correlations are studied within Hadron-String-Dynamics (HSD) transport approach to nucleus-nucleus collisions. We consider the measures $\Delta^{K\pi}$ and $\Sigma^{K\pi}$ for kaon and pion multiplicities in Au+Au collisions in a wide range of collision energies and centralities. These strongly intensive measures appear to cancel the participant number fluctuations. This allows to enlarge the centrality window in the analysis of event-by-event fluctuations up to at least of 10% most central collisions. We also present a comparison of the HSD results with the data of NA49 and STAR collaborations. The HSD describes $\Sigma^{K\pi}$ reasonably well. However, the HSD results depend monotonously on collision energy and do not reproduce the bump-deep structure of $\Delta^{K\pi}$ observed from the NA49 data in the region of the center of mass energy of nucleon pair $\sqrt{s_{NN}} = 8 \div 12$ GeV. This fact deserves further studies. The origin of this ‘structure’ is not connected with simple geometrical or limited acceptance effects, as these effects are taken into account in the HSD simulations.

PACS numbers: 12.40.-y, 12.40.Ee

Keywords: event-by-event fluctuations, nucleus-nucleus collisions

I. INTRODUCTION

A possibility to observe signatures of the critical point of QCD matter inspired the energy and system size scan programs of the NA61 collaboration at the SPS CERN [1] and the low energy scan program of STAR and PHENIX collaborations at the RHIC BNL [2]. These experimental studies focus on the event-by-event (e-by-e) fluctuation measurements in nucleus-nucleus (A+A) collisions. One should compare the fluctuation properties of hadrons produced in collisions of different nuclei at different collision energies. In these reactions the average sizes of the created physical systems and their e-by-e fluctuations are rather different [3]. The fluctuations of the system volume strongly affect the observed hadron fluctuations, i.e. the measured hadron fluctuations do not describe the physical properties of the system but rather reflect the system size fluctuations. In A+A collisions with different centralities a system volume is indeed changed significantly from interaction to interaction. These event-by-event volume variations of the produced matter are usually out of the experimental control.

We recall that extensive quantities are proportional to the system volume V , whereas intensive quantities do not. They are used to describe the local properties of a physical system. In particular, an equation of state of the matter is usually formulated in terms of the intensive physical quantities, e.g., the pressure is considered as a function of temperature and chemical potentials.

In statistical physics a mean value $\langle N \rangle$ of a fluctuating number of particles is an extensive quantity, i.e., $\langle N \rangle \propto V$, whereas the ratio of mean multiplicities of two different particle types is an intensive quantity. If local properties of the system remain unchanged¹, this ratio does not depend on the average size of the system and of its fluctuations. Particle number fluctuations are quantified by the variance, $\text{Var}(N) = \langle N^2 \rangle - \langle N \rangle^2$, which is an extensive quantity in statistical models, while the scaled variance, $\omega_N = [\langle N^2 \rangle - \langle N \rangle^2] / \langle N \rangle$, is an intensive one. However, the scaled variance being an intensive quantity depends on the system size fluctuations.

In the event-by-event analysis of A+A collisions the number of nucleon participants N_{part} and the scaled variance of its fluctuations ω_{part} play the same role as the volume and volume

¹ This is approximately valid in a wide range of centralities, and violated only for very peripheral collision events [4].

fluctuations in statistical models. For example, the fluctuations of nucleon participants strongly contribute to the scaled variances of charged particles [5], pions and kaons [3]. To avoid these unnecessary contributions one needs to make a very rigid centrality selection. The analysis of the scaled variances has to be limited to about 1% most central events only (see, e.g., Ref. [6]). This causes two problems. First, there are technical problems with a strict centrality selection. Second, for a more rigid centrality trigger one evidently loses the number of collision events and thus needs to enlarge strongly the total event statistics.

The analysis of fluctuations of hadron production properties in collisions of relativistic nuclei may profit from the use of measurable intensive quantities which are independent of both the average size of the system and of the size variations. Two families of these quantities – referred to as strongly intensive ones – have been recently proposed in Ref. [7]. In the present study we consider the properties of these strongly intensive measures for particle number fluctuations in A+A collisions within the Hadron-String-Dynamics (HSD) transport approach [8]. We use HSD as it describes well the particle spectra in heavy ion experiments. The large fluctuations of nucleon participants number is under theoretical control. Within the HSD simulations we can estimate and separate these unnecessary fluctuations. Besides, we can check whether these system size fluctuations are really cancelled out in strongly intensive measures.

The strongly intensive measures Δ^{AB} and Σ^{AB} [7] can be defined for two arbitrary extensive quantities A and B . To be specific we consider the total hadron multiplicities of charged kaons $K = K^+ + K^-$ and pions² $\pi = \pi^+ + \pi^-$:

$$\Delta^{K\pi} = \frac{1}{\langle K \rangle + \langle \pi \rangle} [\langle \pi \rangle \omega_K - \langle K \rangle \omega_\pi] , \quad (1)$$

$$\Sigma^{K\pi} = \frac{1}{\langle K \rangle + \langle \pi \rangle} [\langle \pi \rangle \omega_K + \langle K \rangle \omega_\pi - 2 (\langle K\pi \rangle - \langle K \rangle \langle \pi \rangle)] , \quad (2)$$

where

$$\omega_K \equiv \frac{\langle K^2 \rangle - \langle K \rangle^2}{\langle K \rangle} , \quad \omega_\pi = \frac{\langle \pi^2 \rangle - \langle \pi \rangle^2}{\langle \pi \rangle} \quad (3)$$

are the scaled variances of the K and π fluctuations.

² Another pair of extensive quantities – particle multiplicity and sum of their transverse momenta modules – within the UrQMD transport model have been recently discussed in Ref. [9]

The paper is organized as follows. In Section II we consider the properties of different fluctuation measures within the model of independent sources. Section III presents the HSD results in A+A collisions. In Section IV a comparison of the HSD results with the available data is presented. A summary in Section V closes the article.

II. MODEL OF INDEPENDENT SOURCES

It is instructive to start from the model of independent sources (MIS) for multi-particle production in A+A collisions. The number of sources in this model changes from event to event. However, the sources are assumed to be statistically identical (i.e., the average properties of all sources are the same) and independent (i.e., there are no correlations between hadrons produced from different sources). The first and the most popular example of the model of independent sources is the Wounded Nucleon Model [12]. In this model, one assumes that A+A collision can be treated as a superposition of independent contributions from each of N_{part} nucleon participants. For example, the kaon and pion multiplicities are the following:

$$K = K_1 + K_2 + \dots + K_{N_{part}} , \quad \pi = \pi_1 + \pi_2 + \dots + \pi_{N_{part}} . \quad (4)$$

The average multiplicities from each source are equal:

$$\langle K_1 \rangle = \langle K_2 \rangle = \dots = \langle K_{N_{part}} \rangle \equiv n_K , \quad \langle \pi_1 \rangle = \langle \pi_2 \rangle = \dots = \langle \pi_{N_{part}} \rangle \equiv n_\pi . \quad (5)$$

Thus, the e-by-e averages of final hadron multiplicities can be obtained as:

$$\langle K \rangle = \sum_{N_{part}} P(N_{part}) \sum_{j=1}^{N_{part}} \langle K_j \rangle = \sum_{N_{part}} P(N_{part}) n_K N_{part} = n_K \cdot \langle N_{part} \rangle , \quad (6)$$

$$\langle \pi \rangle = \sum_{N_{part}} P(N_{part}) \sum_{j=1}^{N_{part}} \langle \pi_j \rangle = \sum_{N_{part}} P(N_{part}) n_\pi N_{part} = n_\pi \cdot \langle N_{part} \rangle , \quad (7)$$

where $\langle N_{part} \rangle$ is the average number of nucleon participants (i.e., wounded nucleons). The quantities n_K and n_π in Eqs. (6,7) are the average multiplicities per one nucleon participant.

For the second moment of kaon multiplicity distributions one obtains:

$$\langle K^2 \rangle = \sum_{N_{part}} P(N_{part}) \left\langle \left(\sum_{i=1}^{N_{part}} K_i \right)^2 \right\rangle = \sum_{N_{part}} P(N_{part}) \left[\sum_{i=1}^{N_{part}} \langle K_i^2 \rangle + \sum_{1 \neq i < j \leq N_{part}} \langle K_i K_j \rangle \right] . \quad (8)$$

The right hand side of Eq. (8) is a sum of the N_{part}^2 terms $\langle K_i K_j \rangle$. The number of terms with $i = j$ is N_{part} , and the number of ones with $i \neq j$ is $N_{part}^2 - N_{part}$. The different sources are assumed to be statistically identical, i.e. the second moments of kaon number distributions from the different sources are equal to each other:

$$\langle K_i^2 \rangle = \langle K_1^2 \rangle , \quad (9)$$

with $i = 2, \dots, N_{part}$. The different sources are also assumed to be independent, i.e. the kaon-pion pairs emitted by different sources are uncorrelated. This gives for $i \neq j$:

$$\langle K_i K_j \rangle = \langle K_i \rangle \langle K_j \rangle = n_K^2 . \quad (10)$$

From the above equations one finds:

$$\langle K^2 \rangle = \langle K_1^2 \rangle \langle N_{part} \rangle + n_K^2 \left[\langle N_{part}^2 \rangle - \langle N_{part} \rangle \right] . \quad (11)$$

Similarly, one obtains for pions:

$$\langle \pi^2 \rangle = \langle \pi_1^2 \rangle \langle N_{part} \rangle + n_\pi^2 \left[\langle N_{part}^2 \rangle - \langle N_{part} \rangle \right] . \quad (12)$$

For the kaon-pion correlations one finds

$$\langle K_i \pi_i \rangle = \langle K_1 \pi_1 \rangle \quad (13)$$

for $i = 2, \dots, N_{part}$, and

$$\langle K_i \pi_j \rangle = n_K n_\pi \quad (14)$$

for $i \neq j$. It then follows:

$$\langle K \pi \rangle = \langle K_1 \pi_1 \rangle \langle N_{part} \rangle + n_K n_\pi \left[\langle N_{part}^2 \rangle - \langle N_{part} \rangle \right] . \quad (15)$$

The scaled variances for the production of kaons and pions in MIS are then presented as:

$$\omega_K = \omega_K^* + n_K \omega_{part} , \quad \omega_\pi = \omega_\pi^* + n_\pi \omega_{part} , \quad (16)$$

where ω_K^* and ω_π^* are, respectively, the scaled variances of kaons and pions from one source,

$$\omega_K^* = \frac{\langle K_1^2 \rangle - \langle K_1 \rangle^2}{\langle K_1 \rangle} , \quad \omega_\pi^* = \frac{\langle \pi_1^2 \rangle - \langle \pi_1 \rangle^2}{\langle \pi_1 \rangle} , \quad (17)$$

and ω_{part} is the scaled variance of e-by-e fluctuations of the number of nucleon participants,

$$\omega_{part} = \frac{\langle N_{part}^2 \rangle - \langle N_{part} \rangle^2}{\langle N_{part} \rangle} . \quad (18)$$

Similar to Eq. (16) one finds within MIS,

$$\frac{\langle K \pi \rangle - \langle K \rangle \langle \pi \rangle}{\langle K + \pi \rangle} = \frac{\rho_{K\pi}^*}{n_K + n_\pi} + \frac{n_K n_\pi}{n_K + n_\pi} \omega_{part} , \quad (19)$$

where

$$\rho_{K\pi}^* \equiv \langle K_1 \pi_1 \rangle - \langle K_1 \rangle \langle \pi_1 \rangle \quad (20)$$

describes the correlations between K and π numbers in one source.

In MIS, the scaled variances ω_K and ω_π (16) are independent of the average number of nucleon participants $\langle N_{part} \rangle$. Thus, ω_K and ω_π are intensive quantities. However, they depend on the fluctuations of the number of nucleon participants via ω_{part} and, therefore, they are not strongly intensive quantities. From above formulas it follows that both measures Δ (1) and Σ (2) are strongly intensive quantities within the MIS, i.e. they are independent of $\langle N_{part} \rangle$ and of ω_{part} :

$$\Delta^{K\pi} = \frac{1}{n_K + n_\pi} [n_\pi \omega_K^* - n_K \omega_\pi^*] , \quad (21)$$

$$\Sigma^{K\pi} = \frac{1}{n_K + n_\pi} [n_\pi \omega_K^* + n_K \omega_\pi^* - 2\rho_{K\pi}^*] . \quad (22)$$

The contributions from nuclear participants can be obtained from nucleon-nucleon collisions which should be considered as the properly weighted sum of p+p, p+n, and n+n interactions [13]. At high SPS and RHIC energies the results in nucleon-nucleon collisions are close to those in p+p collisions. Thus, in the above equations one may approximate the MIS quantities with the results of p+p inelastic interactions at the same collision energy per nucleon. Inelastic p+p collisions might be understood within MIS as the system with $N_{part} = 2$ and $\omega_{part} = 0$. It then follows:

$$n_K \cong \frac{1}{2} \langle K \rangle_{pp} , \quad n_\pi \cong \frac{1}{2} \langle \pi \rangle_{pp} , \quad \rho_{K\pi}^* \cong \frac{1}{2} [\langle K \pi \rangle_{pp} - \langle K \rangle_{pp} \langle \pi \rangle_{pp}] , \quad (23)$$

$$\omega_K^* \cong \frac{\langle K^2 \rangle_{pp} - \langle K \rangle_{pp}^2}{\langle K \rangle_{pp}} , \quad \omega_\pi^* \cong \frac{\langle \pi^2 \rangle_{pp} - \langle \pi \rangle_{pp}^2}{\langle \pi \rangle_{pp}} , \quad (24)$$

i.e., particle multiplicities n_K and n_π , and K - π -correlations $\rho_{K\pi}^*$ from one source are equal to one half of those values in p+p collisions, whereas the scaled variances ω_K^* and ω_π^* for one source coincide with the corresponding scaled variances in p+p collisions.

Another interpretation of MIS can be obtained in terms of the statistical mechanics. One may assume that the matter created in A+A collisions at different centralities corresponds to systems in statistical equilibrium with the same temperature and chemical potentials, but with a volume varying from event to event. It is also natural to assume that the volume is proportional to the number of nucleon participants $V \propto N_{part}$. One then finds [7] within the grand canonical ensemble formulation a validity of Eqs. (21) and (22). In this case, the hadron multiplicities n_K and n_π , scaled variances ω_K^* and ω_π^* , and correlation $\rho_{K\pi}^*$ should be found as the corresponding quantities at fixed volume (i.e., at fixed N_{part}). The transport model calculations demonstrate [3] that the e-by-e fluctuations of the number of participants become negligible in the sample of most central A+A collisions, e.g., one finds $\omega_{part} \ll 1$ in Pb+Pb (or Au+Au) collisions with impact parameter equal to zero, $b = 0$. Therefore, one may define the parameters of MIS as:

$$n_K = \frac{\langle K \rangle_{b=0}}{\langle N_{part} \rangle_{b=0}}, \quad n_\pi = \frac{\langle \pi \rangle_{b=0}}{\langle N_{part} \rangle_{b=0}}, \quad \rho_{K\pi}^* \cong \frac{\langle K\pi \rangle_{b=0} - \langle K \rangle_{b=0} \langle \pi \rangle_{b=0}}{\langle N_{part} \rangle_{b=0}}, \quad (25)$$

$$\omega_\pi^* \cong \omega_\pi(b=0), \quad \omega_K^* \cong \omega_K(b=0), \quad (26)$$

i.e., particle multiplicities n_K and n_π , and K - π -correlations $\rho_{K\pi}^*$ are equal to the results in A+A collisions with zero impact parameter divided by the average number of nucleon participants at $b = 0$. On the other hand, the scaled variances ω_K^* and ω_π^* entering in MIS results just coincide with the corresponding scaled variances in A+A collisions at $b = 0$.

Another quantity frequently used to characterize the fluctuations of K and π particle numbers is [11]:

$$\nu_{dyn}^{K\pi} \equiv \frac{\langle K(K-1) \rangle}{\langle K \rangle^2} + \frac{\langle \pi(\pi-1) \rangle}{\langle \pi \rangle^2} - 2 \frac{\langle K\pi \rangle}{\langle K \rangle \langle \pi \rangle}. \quad (27)$$

One can easily find the relation:

$$\nu_{dyn}^{K\pi} = \frac{\langle K + \pi \rangle}{\langle K \rangle \langle \pi \rangle} [\Sigma^{K\pi} - 1]. \quad (28)$$

Equation (28) shows that ν_{dyn}^{AB} , similar to Σ^{AB} , is independent of fluctuations of the number of participants, but it decreases as $\nu_{dyn}^{AB} \propto \langle N_{part} \rangle^{-1}$ and, thus, it is not an intensive quantity.

We prefer to use the strongly intensive quantities and will compare the HSD results with the data on ν_{dyn} but recalculated in Σ according to Eq. (28).

III. THE RESULTS OF HADRON-STRING-DYNAMICS

In order to study the properties of strongly intensive measures (1) and (2) we calculate the fluctuations of kaon and pion numbers with the HSD transport approach [8]. First, we consider the centrality dependence in A+A collisions. The HSD results in Au+Au collisions at the center of mass energy of the nucleon pair $\sqrt{s_{NN}} = 7.7$ GeV ($E_{lab} \simeq 30$ AGeV) are presented in Fig. 1.

The collision energy is chosen in the region where the NA49 Collaboration observes the horn structure [14]. The squares and circles show the HSD results for pions and kaons, respectively, at different impact parameters b . The stars present the HSD results for ω_{part} (18) which correspond to the fluctuation of the number of nucleon participants. The lines are the results of the MIS. We consider two version of MIS based on Eqs. (23,24) and Eqs. (25,26), respectively, as discussed in the previous section. The parameters n_π , n_K , ω_π^* , ω_K^* , and $\rho_{K\pi}^*$ are thus taken from the results of p+p collisions (23,24) and from the HSD results at $b = 0$ (25,26). These MIS results will be denoted as MIS(pp) and MIS($b = 0$), respectively. The MIS($b = 0$) calculations assume that $\omega_{part} \cong 0$ at $b = 0$. This is indeed supported by the HSD results presented in Fig. 1(b). The MIS parameters (23,24) or (25,26) are then used at all impact parameters b . The average number of participants $\langle N_{part} \rangle$ and its fluctuations ω_{part} are found for different values of $b \geq 0$ from the HSD simulations. Fig. 1(a) demonstrates the ratios $\langle \pi \rangle / \langle N_{part} \rangle$ and $\langle K \rangle / \langle N_{part} \rangle$ as functions of b . One observes a slight decrease of pion and kaon multiplicities per participating nucleon with increasing b . On the other hand, the fluctuations of N_{part} strongly increase with b as seen from Fig. 1(b). Thus according to the MIS formula (16) one may expect an increase of $\omega_K(b)$ and $\omega_\pi(b)$ as functions of b . This is indeed observed in Fig. 1(c) and Fig. 1(d). The MIS lines in Fig. 1(c) and (d) give a correct qualitative description of the HSD results for the pion and kaon multiplicity fluctuations at different centralities in Au+Au collisions (more details on the connection of the model of independent sources and HSD results for the e-by-e fluctuations can be found in Ref. [3]). Note that the results of MIS(pp) and

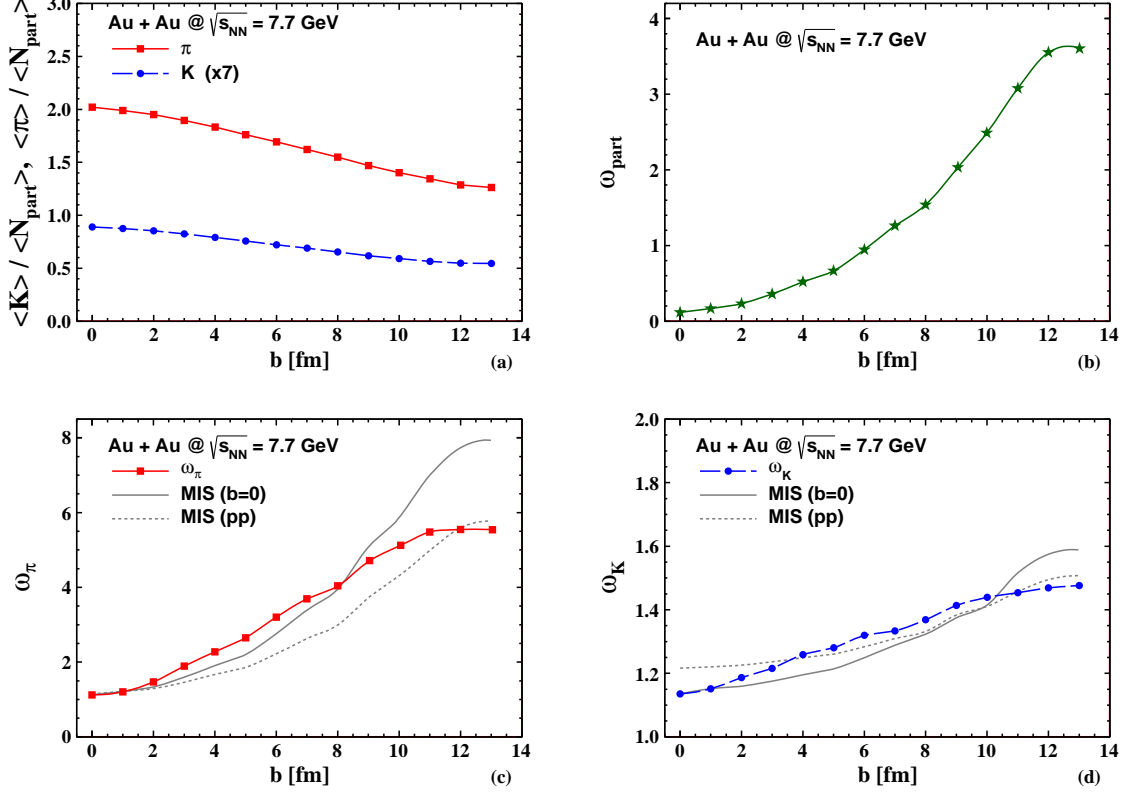


FIG. 1: The symbols correspond to the HSD results at different impact parameter b in Au+Au collisions at $\sqrt{s_{NN}} = 7.7$ GeV. (a): The HSD ratio of pion and kaon multiplicities to the average number of participants. Note that $\langle K \rangle / \langle N_{part} \rangle$ is multiplied by a factor of 7. (b): The scaled variance ω_{part} . (c): The scaled variance ω_{π} . (d): The scaled variance ω_K . The solid and dotted lines in (c) and (d) show the MIS($b = 0$) and MIS(pp) results, respectively.

MIS($b = 0$) are rather close to each other. As the parameters (25,26) are fixed according to the HSD at $b = 0$, the MIS($b = 0$) lines coincide, by construction, with the HSD results at $b = 0$. The b -dependence of the MIS results is fully defined by the b -dependence of $\langle N_{part} \rangle$ and ω_{part} . Consequently, one may conclude that a strong rise in the scaled variances ω_{π} and ω_K with b seen in Fig. 1(c) and Fig. 1(d) is caused by an increase of the e-by-e fluctuations of N_{part} with increasing b .

The participant number fluctuations are, however, cancelled out in the strongly intensive measures. Therefore, $\Delta^{K\pi}$ (1) and $\Sigma^{K\pi}$ (2) demonstrate only a very weak b -dependence as seen

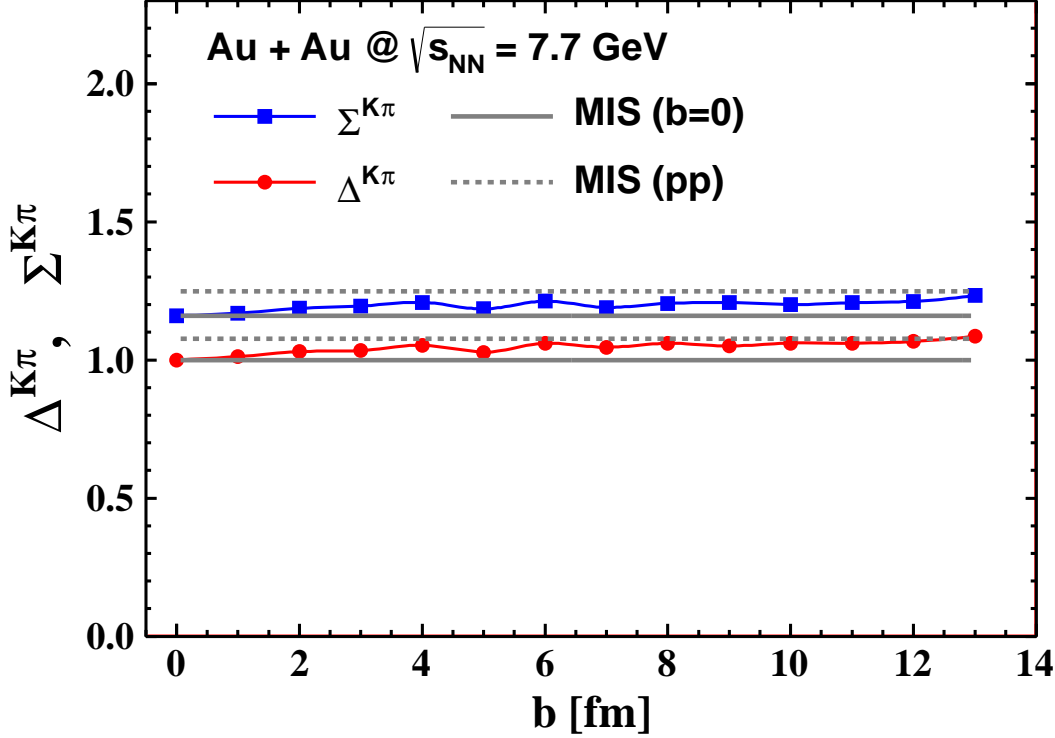


FIG. 2: The strongly intensive measures $\Delta^{K\pi}$ (circles) and $\Sigma^{K\pi}$ (squares). The symbols correspond to the HSD results for Au+Au collisions at $\sqrt{s_{NN}} = 7.7$ GeV. The horizontal solid lines show the MIS($b = 0$) results for $\Delta^{K\pi}$ and $\Sigma^{K\pi}$. The horizontal dotted lines show the MIS(pp) results. The lower lines correspond to $\Delta^{K\pi}$ and the upper lines to $\Sigma^{K\pi}$.

in Fig. 2. Note that the MIS results (21,22) do not depend on $\langle N_{part} \rangle$ and on ω_{part} . Therefore, the MIS results correspond to the values of Σ and Δ which are independent of impact parameter b . These MIS results are presented by the horizontal lines in Fig. 2.

The results presented in Figs. 1 and 2 remain qualitatively the same at higher collision energies. In Fig. 3 and 4 we present the corresponding results in Au+Au collisions at the highest RHIC energy $\sqrt{s_{NN}} = 200$ GeV. The kaon $\langle K \rangle / \langle N_{part} \rangle$ and pion $\langle \pi \rangle / \langle N_{part} \rangle$ multiplicities per participating nucleon increase with collision energy. As seen from Fig. 3(a), these values at $\sqrt{s_{NN}} = 200$ GeV are approximately 5 and 10 times larger than the corresponding values at $\sqrt{s_{NN}} = 7.7$ GeV presented in Fig. 1(a). The MIS thus predicts a much stronger increase of ω_K and ω_π with b at high collision energy. The HSD results presented in Figs. 3(c) and 3(d)

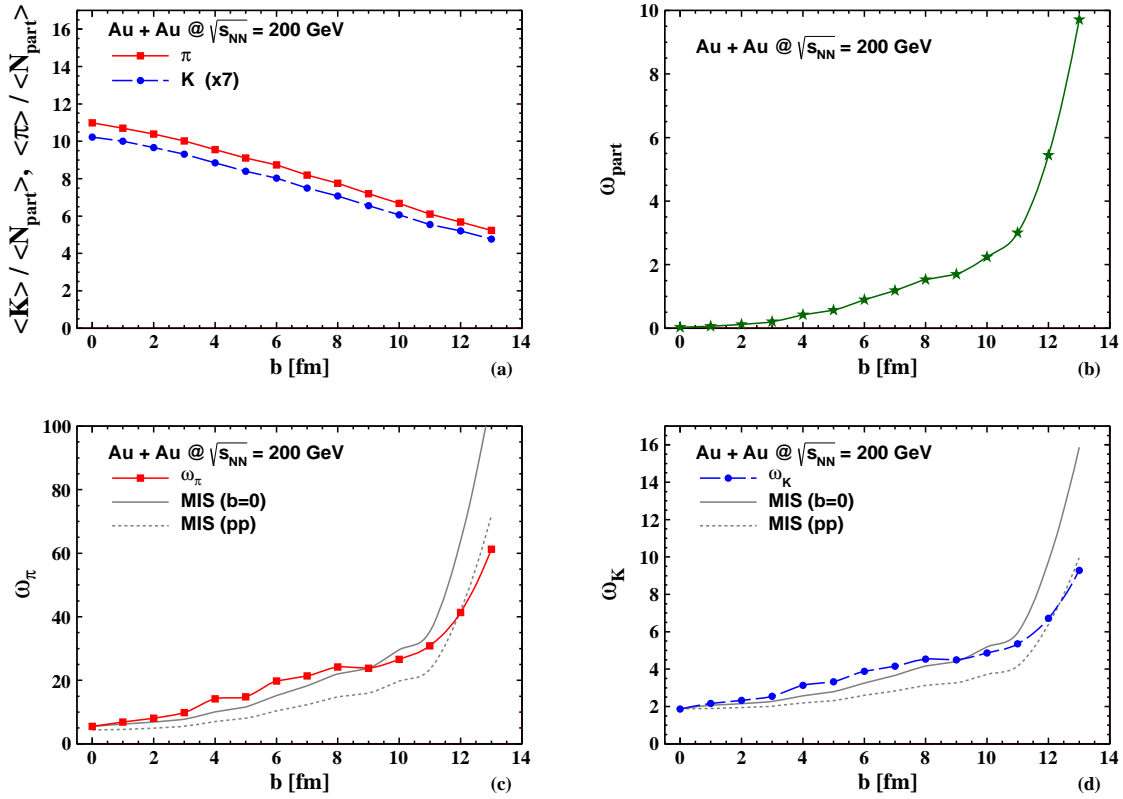


FIG. 3: The same as in Fig. 1 but for $\sqrt{s_{NN}} = 200$ GeV.

support these expectations. One observes also an increase of ω_K^* and ω_{π}^* with $\sqrt{s_{NN}}$ reported earlier in Ref. [13].

The results presented in Fig. 1 and Fig. 3 lead to the conclusion that the fluctuation measures ω_{π} and ω_K are useless for the samples of A+A collision events within wide centrality windows because of large fluctuations of the number of participants. For example, in a sample of minimum bias A+A collision events one would obtain very large values of the scaled variances ω_K and ω_{π} . However, the dominant contributions to these values of the scaled variances come evidently from the participant number fluctuations. Indeed, the HSD results correspond to a huge value of $\omega_{part} \approx 100$ in a sample of the minimum bias Au+Au (or Pb+Pb) collisions. Thus, for i th hadron species (e.g., $i = \pi, K$) very large contributions $n_i \omega_{part}$ come to ω_i . These contributions increase with collision energies due to an increase of n_i . On the other hand, the contributions of participant number fluctuations are approximately cancelled out in (1) and (2), and the strongly intensive measures Δ and Σ are expected to remain close to their numerical

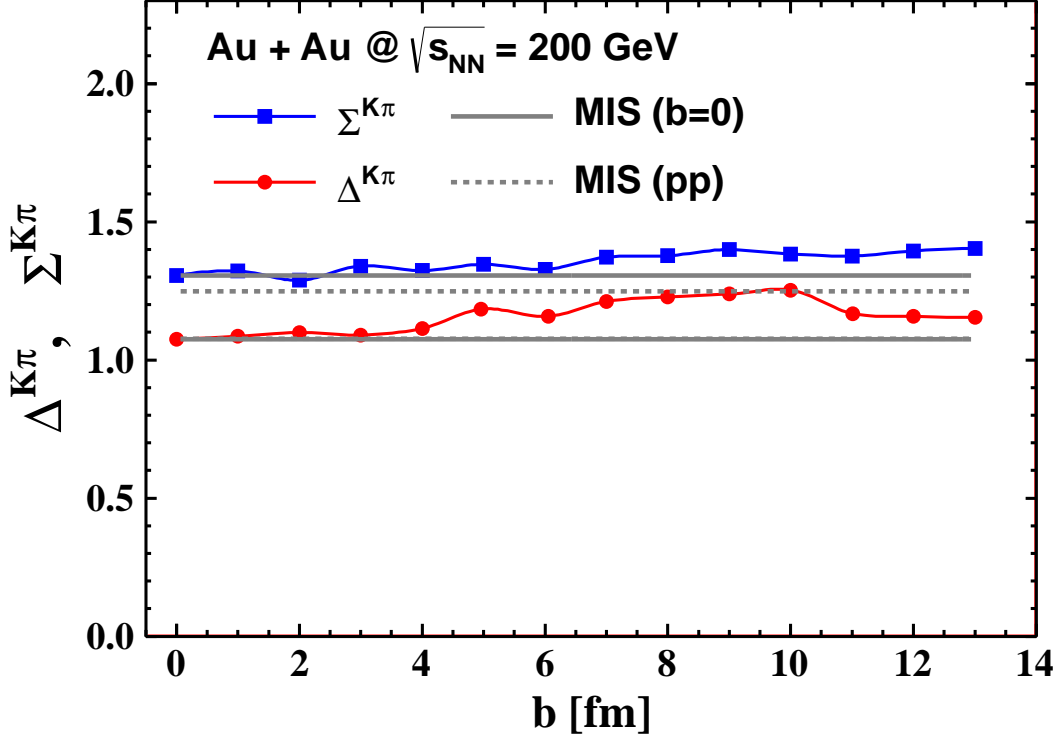


FIG. 4: The same as in Fig. 2 but for $\sqrt{s_{NN}} = 200$ GeV.

values at $b = 0$. This expectation is supported by the HSD results presented in Figs. 2 and 4.

As a further test we perform the HSD simulations in Au+Au collisions at different collision energies for $b \leq 4$ fm. This requirement corresponds approximately to 10% of the most central collisions. For the sample of collision events with $b \leq 4$ fm, the dependence on collision energy of relative multiplicities $\langle \pi \rangle / \langle N_{part} \rangle$ and $\langle K \rangle / \langle N_{part} \rangle$, and scaled variance ω_{part} is shown in Fig. 5(a) and 5(b), respectively. In Fig. 6 the HSD results are presented for the scaled variances of ω_K and ω_π as a function of the collision energy $\sqrt{s_{NN}}$. The calculations in Au+Au collisions for $b \leq 4$ fm are compared to those for $b = 0$ and to the results of MIS. The main features of the results for the scaled variances ω_π and ω_K presented in Fig. 6 can be summarized as follows: An averaging over Au+Au collision events with $b \leq 4$ fm leads to very strong increase of ω_π and ω_K in a comparison to their values at $b = 0$. For example, at $\sqrt{s_{NN}} = 200$ GeV the scaled variance ω_π for $b \leq 4$ fm is higher than ω_π for $b = 0$ by approximately a factor of 10. As seen from Fig. 6, the MIS results explain only a part of this increase.

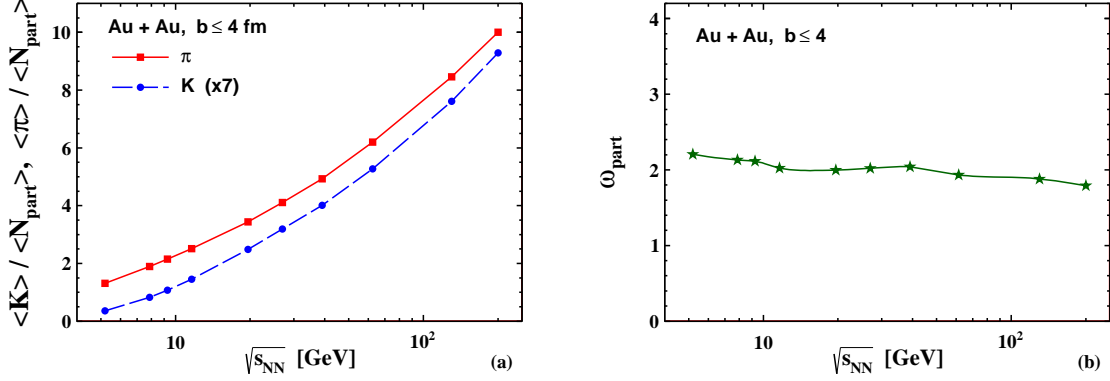


FIG. 5: The HSD results in Au+Au collisions for $b \leq 4$ fm as a function of the center of mass energy per nucleon pair $\sqrt{s_{NN}}$. (a): The values of relative particle multiplicities per participating nucleon $\langle K \rangle / \langle N_{part} \rangle$ and $\langle \pi \rangle / \langle N_{part} \rangle$. Note that $\langle K \rangle / \langle N_{part} \rangle$ is multiplied by a factor of 7. (b): The scaled variances ω_{part} .

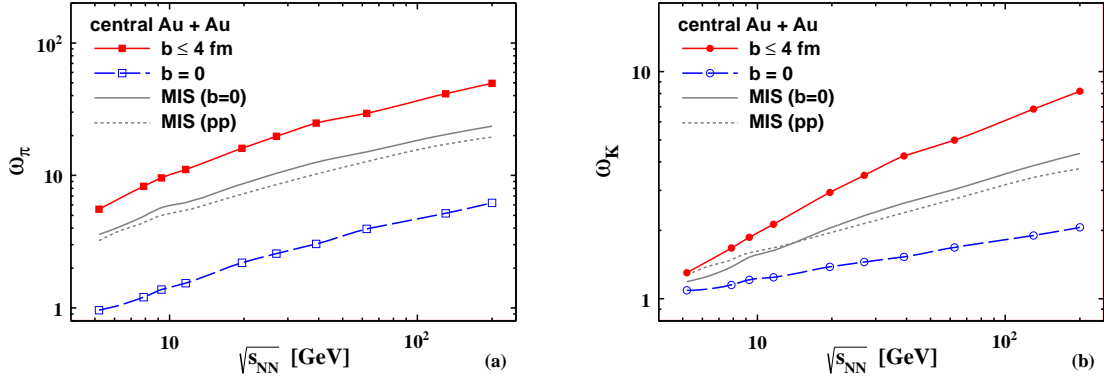


FIG. 6: The HSD results for the scaled variances ω_π (a) and ω_K (b) in Au+Au collisions at $b = 0$ (open symbols) and at $b \leq 4$ fm (full symbols). The solid and dotted lines show the MIS($b=0$) and MIS(pp) results, respectively.

The contributions from participant number fluctuations are quite strong in the sample of Au+Au collision events with $b \leq 4$ fm. These contributions are, however, cancelled out in the strongly intensive measures $\Delta^{K\pi}$ (1) and $\Sigma^{K\pi}$ (2). These measures for the sample $b \leq 4$ fm remain close to their numerical values at $b = 0$. This is shown in Fig. 7. Note that the MIS($b = 0$) results for $\Delta^{K\pi}$ and $\Sigma^{K\pi}$ in the sample of $b \leq 4$ fm are identical to those at $b = 0$.

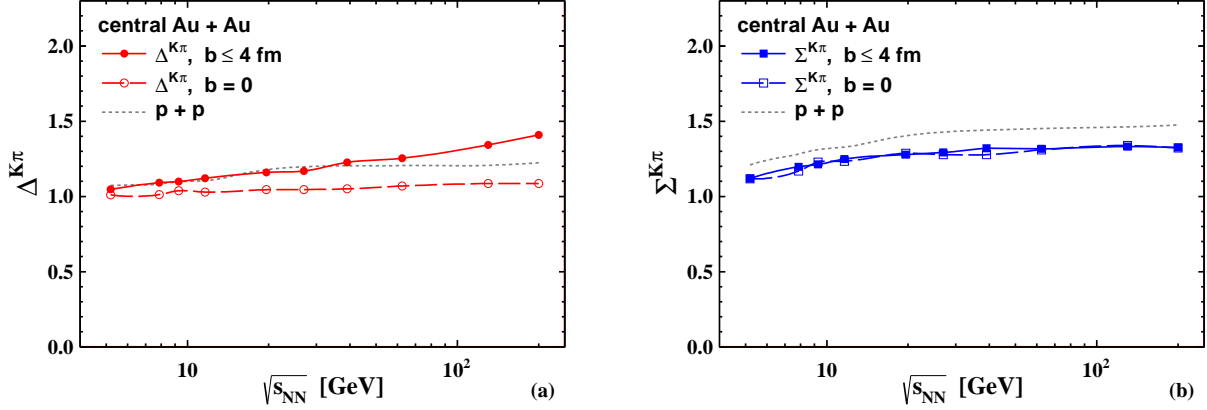


FIG. 7: The HSD results for the strongly intensive measures $\Delta^{K\pi}$ and $\Sigma^{K\pi}$ in Au+Au collisions at $b = 0$ (open symbols) and at $b \leq 4$ fm (full symbols). The lower and upper dotted lines show the MIS(pp) results for $\Delta^{K\pi}$ and $\Sigma^{K\pi}$, respectively.

Therefore, only the p+p HSD results are presented in Fig. 7 by the dotted lines. Figure 7(b) shows that $\Sigma^{K\pi}(b \leq 4 \text{ fm}) \cong \Sigma^{K\pi}(b = 0)$. On the other hand, an increase of about 30% at the highest RHIC energy $\sqrt{s_{NN}} = 200$ GeV is seen in Fig. 7(a) for $\Delta^{K\pi}$ for the sample of $b \leq 4$ fm in comparison to that at $b = 0$.

IV. COMPARISON TO THE NA49 AND STAR DATA

In this section we present a comparison of the HSD results for the strongly intensive measures $\Delta^{K\pi}$ and $\Sigma^{K\pi}$ with existing data on e-by-e fluctuations.

Recently the NA49 Collaboration published the data on mean multiplicities, correlations and fluctuations of pions, kaons and protons in Pb+Pb collisions [15]. From these data we are able to construct the fluctuation measure $\Delta^{K\pi}$ and $\Sigma^{K\pi}$. The STAR Collaboration has published only the data for ν_{dyn} [16] in Au+Au collisions. We manage to recalculate them into Σ values using Eq. (28) and the preliminary data on mean multiplicities of kaons and pions [17].

The results for $\Delta^{K\pi}$ in the SPS energy region are presented in Fig. 8. The squares present the NA49 results for 3.5% most central Pb+Pb collisions. One can see that the NA49 data for $\Delta^{K\pi}$ show a non-monotonous behavior with a bump at $\sqrt{s_{NN}} = 8.8$ GeV and a deep at $\sqrt{s_{NN}} = 12.3$ GeV. The NA49 Collaboration did not yet publish the error-bars for the first

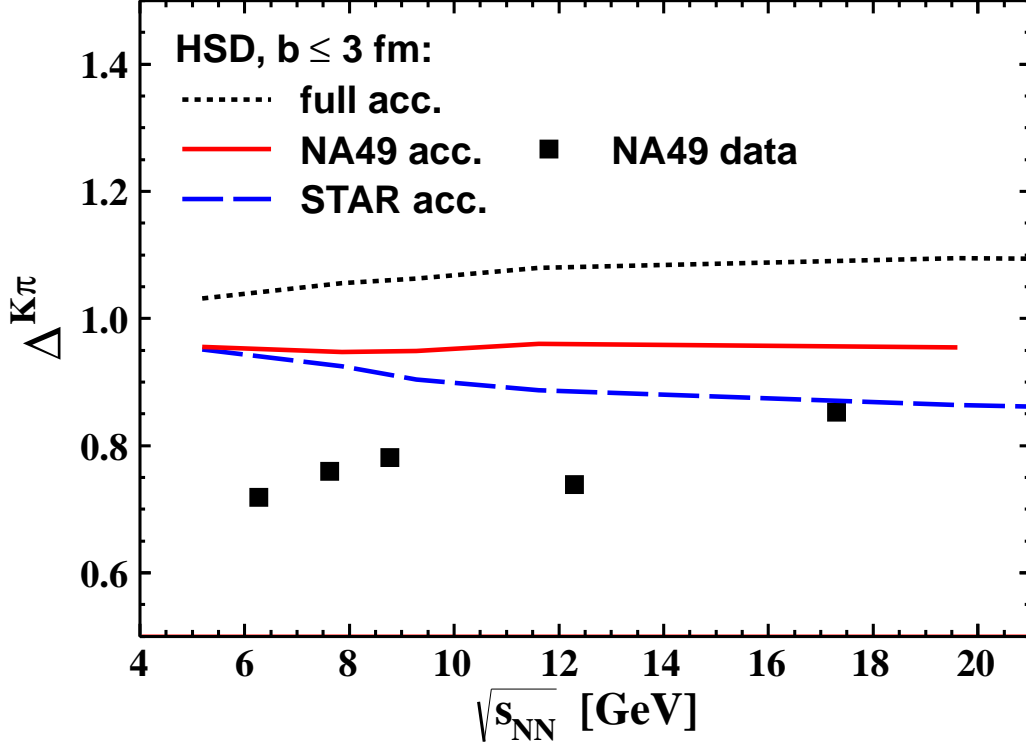


FIG. 8: The squares are the NA49 data for $\Delta^{K\pi}$ for 3.5% most central Pb+Pb collisions. The solid, dashed, and dotted lines show the HSD results in Au+Au collisions at $b \leq 3$ fm within the NA49, STAR, and full 4π acceptances, respectively.

and second moments of K and π multiplicity distributions. Therefore, it is difficult to conclude whether the non-monotonous structure in $\Delta^{K\pi}$ has a real statistical significance. However, this potential irregularity happens in the energy range where other signals of unusual behavior (*kink*, *horn*, *step*) were observed by the NA49 Collaboration [14]. It would be interesting to see the STAR data for $\Delta^{K\pi}$ in this energy range.

The results for $\Sigma^{K\pi}$ are presented in Fig. 9. The squares correspond to the NA49 data and the stars to the STAR data. The available error-bars for $\nu_{dyn}^{K\pi}$ can be used for a rough estimate of the error-bars for $\Sigma^{K\pi}$. These error-bars seem to be quite small and comparable with the size of the star-symbols in Fig. 9.

The NA49 and STAR Collaborations have different colliding nuclei (Pb+Pb and Au+Au, respectively), different acceptances and different centralities (3.5% and 5% most central colli-

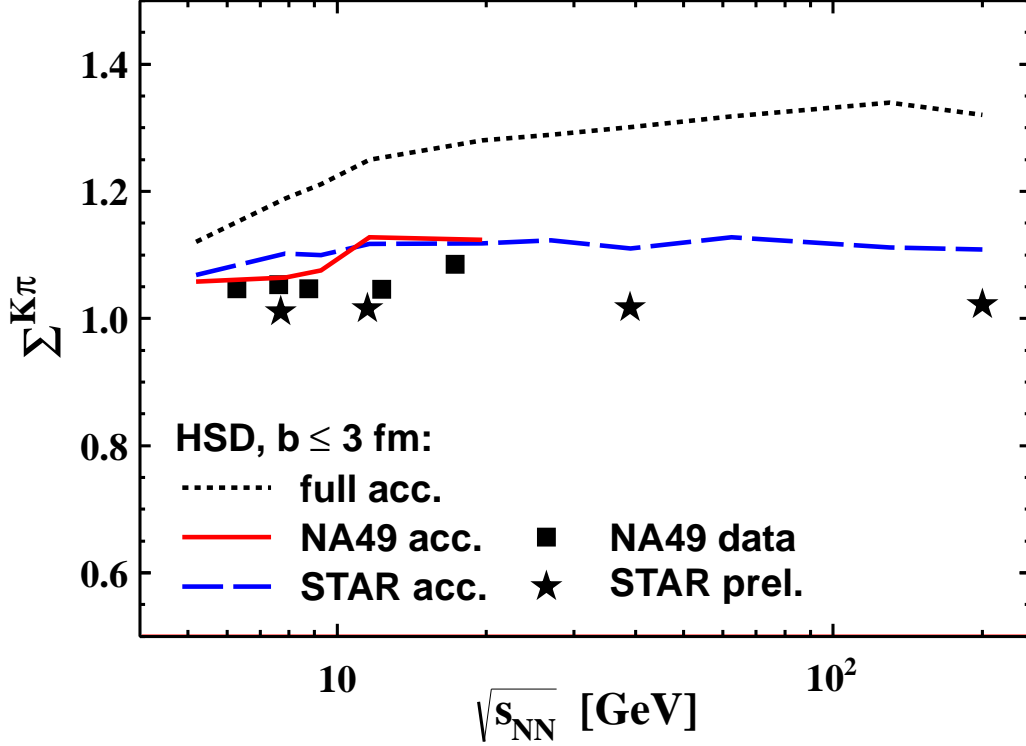


FIG. 9: The squares are the NA49 data for $\Sigma^{K\pi}$ for 3.5% most central Pb+Pb collisions, and the stars are the STAR data for 5% most central Au+Au collisions. The solid, dashed, and dotted lines show the HSD results in Au+Au collisions at $b \leq 3$ fm within the NA49, STAR, and full 4π acceptances, respectively.

sions, respectively). We restrict our HSD simulations to impact parameters $b \leq 3$ in Au+Au collisions. This corresponds approximately to 5% most central events. We use this centrality criterion for both NA49 and STAR data, as the quantities $\Delta^{K\pi}$ and $\Sigma^{K\pi}$ are only weakly dependent on centrality selection. However, we take into account the exact experimental acceptances which are different for the NA49 and STAR data. In Figs. 8 and 9 the HSD results are shown by the solid and dashed lines for the NA49 and STAR acceptances, respectively. The HSD results in the full 4π -acceptance are shown by the dotted lines. A presence of the dashed lines in Figs. 8 and 9 helps to estimate the effects of the limited acceptances in NA49 and STAR experiments.

As seen in Figs. 8 and 9 the HSD results correspond to higher values of $\Delta^{K\pi}$ and $\Sigma^{K\pi}$

than their experimental estimates. This is especially seen for $\Delta^{K\pi}$. The HSD results depend monotonously on collision energy and can not explain the bump(deep) in the NA49 data for $\Delta^{K\pi}$. Therefore, the origin of this ‘bump’ (if it will survive in future measurements) is not connected with simple geometrical or limited acceptance effects, as these effects are taken into account in the HSD simulations.

V. SUMMARY

The recently proposed two families of strongly intensive measures of fluctuations and correlations are studied within the HSD transport approach to nucleus-nucleus collisions. We test the measures $\Delta^{K\pi}$ (1) and $\Sigma^{K\pi}$ (2) for the fluctuations of kaon and pion numbers in Au+Au collisions at different collision energies and different centralities.

The conventional measures like scaled variances ω_K and ω_π become useless for wide centrality samples because of the dominant contribution from the participant number fluctuations. This fact required a very rigid centrality selection like 1% most central Pb+Pb collision events in Ref. [6]. The other popular measure, ν_{dyn} , is independent of participant number fluctuations, but depends on the average number of participants. Therefore, ν_{dyn} is inconvenient for comparison of p+p and Au+Au collisions as well as for the search for the QCD critical point by system size scan program of NA61 Collaboration at the CERN SPS.

The quantities $\Delta^{K\pi}$ and $\Sigma^{K\pi}$ appear to be useful measures of chemical fluctuations in the wide centrality samples of collision events. In the sample of 10% most central Au+Au collision events we find that $\Delta^{K\pi}$ is slightly larger than that at $b = 0$, and $\Sigma^{K\pi}$ is approximately equal to its value at zero impact parameter $b = 0$. This makes $\Delta^{K\pi}$ and $\Sigma^{K\pi}$ rather helpful in studies of event-by-event fluctuations in nucleus-nucleus collisions. Combining existing experimental data of NA49 and STAR Collaborations on K - π fluctuations and correlations we have obtained $\Delta^{K\pi}$ and $\Sigma^{K\pi}$ and compared them to the corresponding HSD calculations. The data on $\Sigma^{K\pi}$ depend monotonously on the collision energy, whereas $\Delta^{K\pi}$ from the NA49 data has a little bump(deep) in the region $\sqrt{s_{NN}} \cong 8 \div 12$ GeV, where other signals of irregular behavior of physical quantities were previously reported [14]. The HSD describes $\Sigma^{K\pi}$ reasonably well, but does not reproduce the behavior of $\Delta^{K\pi}$. The data analyzed in the present paper correspond

to $3 \div 5\%$ most central collisions. This centrality window can be enlarged at least to 10% in the future experimental studies using strongly intensive measures $\Delta^{K\pi}$ and $\Sigma^{K\pi}$.

Acknowledgments

We are thankful to W. Cassing, M. Gaździcki, K. Grebieszko, W. Greiner, M. Maćkowiak, A. Rustamov, and T. Tarnowsky, for fruitful discussions and comments. E.L.B. and V.V.B. acknowledge the financial support through the "HIC for FAIR" framework of the "LOEWE" program. V.V.B. and V.P.K. acknowledge also the financial support from the DFG foundation. The work of M.I.G. was supported by the Humboldt Foundation and by the Program of Fundamental Research of the Department of Physics and Astronomy of NAS, Ukraine.

-
- [1] M. Gazdzicki [NA61/SHINE Collaboration], J. Phys. G **36**, 064039 (2009).
 - [2] G. Odyniec [STAR Collaboration], J. Phys. G **35**, 104164 (2008); A. Adare *et al.* [PHENIX Collaboration], Phys. Rev. C **78**, 044902 (2008).
 - [3] V. P. Konchakovski, M. I. Gorenstein, E. L. Bratkovskaya, and W. Greiner, J. Phys. G **37**, 073101 (2010).
 - [4] S. Das [STAR Collaboration], arXiv:1210.6099 [nucl-ex]; L. Kumar [STAR Collaboration], arXiv:1211.1350 [nucl-ex].
 - [5] M. M. Aggarwal *et al.* [WA98 Collaboration], Phys. Rev. C **65** (2002) 054912 [nucl-ex/0108029].
 - [6] V. V. Begun, M. Gaździcki, M. I. Gorenstein, M. Hauer, V. P. Konchakovski and B. Lungwitz, Phys. Rev. C **76**, 024902 (2007).
 - [7] M. I. Gorenstein and M. Gazdzicki, Phys. Rev. C **84**, 014904 (2011).
 - [8] W. Ehhalt and W. Cassing, Nucl. Phys. A **602**, 449 (1996) J. Geiss, W. Cassing, and C. Greiner, Nucl. Phys. A **644**, 107 (1998); W. Cassing and E. L. Bratkovskaya, Phys. Rept. **308**, 65 (1999).
 - [9] K. Grebieszko, arXiv:1202.5583 [nucl-th].
 - [10] S. A. Voloshin, V. Koch and H. G. Ritter, Phys. Rev. C **60** (1999) 024901 [nucl-th/9903060].
 - [11] C. Pruneau, S. Gavin and S. Voloshin, Phys. Rev. C **66** (2002) 044904 [nucl-ex/0204011].
 - [12] A. Bialas, M. Bleszynski, and W. Czyz, Nucl. Phys. **B111**, 461 (1976).

- [13] V. P. Konchakovski, M. I. Gorenstein, and E. L. Bratkovskaya, Phys. Lett. B **651**, 114 (2007).
- [14] S. V. Afanasiev *et al.* [The NA49 Collaboration], Phys. Rev. C **66**, 054902 (2002); M. Gaździcki, M.I. Gorenstein, and P. Seyboth, Acta Phys. Polon. B **42**, 307 (2011).
- [15] A. Rustamov, Report from NA49 and NA61/SHINE at the CERN SPS, Proceedings of QM2012.
- [16] T. J. Tarnowsky [STAR Collaboration], Acta Phys. Polon. Supp. **5**, 515 (2012) [arXiv:1201.3336 [nucl-ex]].
- [17] T. J. Tarnowsky, private communications.